



HAL
open science

A Fast and Rigorous Assessment of the Specific Absorption Rate (SAR) for MIMO Cellular Equipment Based on Vector Near-Field Measurements

Mounir Teniou, Ourouk Jawad, Stephane Pannetrat, Lyazid Aberbour

► **To cite this version:**

Mounir Teniou, Ourouk Jawad, Stephane Pannetrat, Lyazid Aberbour. A Fast and Rigorous Assessment of the Specific Absorption Rate (SAR) for MIMO Cellular Equipment Based on Vector Near-Field Measurements. 2020 14th European Conference on Antennas and Propagation (EuCAP), Mar 2020, Copenhagen, Denmark. 10.23919/EuCAP48036.2020.9135506 . hal-02954816v2

HAL Id: hal-02954816

<https://hal.science/hal-02954816v2>

Submitted on 14 Oct 2020

HAL is a multi-disciplinary open access archive for the deposit and dissemination of scientific research documents, whether they are published or not. The documents may come from teaching and research institutions in France or abroad, or from public or private research centers.

L'archive ouverte pluridisciplinaire **HAL**, est destinée au dépôt et à la diffusion de documents scientifiques de niveau recherche, publiés ou non, émanant des établissements d'enseignement et de recherche français ou étrangers, des laboratoires publics ou privés.

A Fast and Rigorous Assessment of the Specific Absorption Rate (SAR) for MIMO Cellular Equipment Based on Vector Near-Field Measurements

Mounir Teniou¹, Ourouk Jawad¹, Stephane Pannetrat¹, Lyazid Aberbour¹

¹ ART-Fi: Orsay, France, e-mail address : mounir.teniou@art-fi.eu, ourouk.jawad@art-fi.eu, stephane.pannetrat@art-fi.eu, lyazid.aberbour@art-fi.eu

Abstract— This paper introduces a rigorous and fast procedure for accurate assessment of the peak averaged specific absorption rate (SAR), quantifying the user exposure to the electromagnetic field radiation from new-radio communication devices. Focus is lent to the specific class of user equipment that exploit multiple-input multiple-output (MIMO) technology and using exclusive simultaneous excitations of the active antenna-array system, such as expected on 5G devices. In contrast with the required $N(N-1)+1$ measurements on traditional SAR systems that only take measurements of the amplitude of the electric field, it is demonstrated in this paper that only $N+1$ number of measurements are required to evaluate the true SAR of a N -antenna MIMO thanks to using a vector near-field based SAR measurement system.

Index Terms—SAR, RF Exposure, MIMO, Planar near field measurement, Vector field measurements, Active-Antenna Measurement.

I. INTRODUCTION

In recent years, communication systems are drastically evolving and increasing in complexity of their communication technologies, especially with the advent of 5G and LTE advanced radios. Of the foundations of these new technologies is the multiple-input multiple-output (MIMO) technology [1], which raises unprecedented challenges in their compliance testing. For an accurate assessment of the specific absorption rate (SAR) compliance [2-3] of a MIMO user-equipment, it is necessary to assess the electromagnetic field (EMF) exposure level from all possible combinations of the antenna-array excitation coefficients [4], hence resulting nowadays in unpractically high-number and time-consuming measurements to be performed. In order to overcome the underlying industrial constraints, especially on the time-to-market delays, several field combining techniques have been introduced in the literature as well as in international standards and guidance [5-7]. The aforementioned combining methods take as input the individual fields radiated by each antenna of the MIMO array, and yield the most accurate SAR results when the EMF-exposure measurement system takes measurements of the complex vector field phasor. In the case of systems that take measurement of only the amplitude of the field, it is demonstrated that the combining methods yield only conservative and inaccurate estimates of the SAR [5].

Recently, D. T. Le, *et al* introduced in [8] methods for MIMO SAR evaluation that are accurate, but time-consuming when applied on traditional SAR systems that take the measurements of the field amplitude only [9]. The lack of phase measurements lead in the proposed method to perform at least $N(N-1)+1$ measurements of the amplitude of field combinations to test a N antenna system. In contrary, in the case of a SAR system capable of measuring both the amplitude and the phase of the complex field phasor, as is the case of ART-MANTM system [10-11], the method enables both accurate and fast test procedure of the MIMO SAR, as only N measurements of the E-field phasor are needed for the evaluation of all possible combinations of the MIMO system.

It should be noted that the method in [8] requires a unique phase reference for all the different N vector-field combination measurements; it is for instance the case of near-field scanning using a vector network analyser for passive antenna testing, where a unique phase reference is provided by the source signal for all the excitation of the antenna array. In the case of active antennas, such as in 5G user equipment, there is no practical access to the RF source, but it is possible to take as a phase reference-wave the time-domain radiofrequency voltages that are induced on a fixed-location probe by the field radiated by the antenna while taking the scan of the field phasor [10-11].

A simple and efficient procedure is introduced in [12] for the MIMO SAR evaluation that incorporates a calibration method of the phase reference of the aforementioned independent N field phasor measurements. It is introduced for the specific case of a MIMO system in which it is possible to individually excite the antenna array elements.

In this paper, a similar procedure is proposed, including the phase calibration method, but for the case of MIMO systems that feature exclusive simultaneous excitations of the antenna array. The proposed procedure is detailed in Section-II, and demonstrated on analytical and experimental results in Section-III.

II. FORMULATION

Let's consider a MIMO system composed of N antenna transmitters (See Fig.1) in the context of SAR measurement.

The local SAR value is defined at each point $P(x, y, z)$ of space as:

$$SAR(x, y, z) = \frac{\sigma |\mathbf{E}(x, y, z)|^2}{2\rho} \left[\frac{\text{W}}{\text{kg}} \right] \quad (1)$$

where σ and ρ are the electric conductivity [S/m] and the mass density [kg/m³] of the homogeneous media simulating the human-tissue used in experimental assessment systems (their values are tabulated as function of the frequency in international standards [2]). $\mathbf{E}(x, y, z)$ is the complex electric-field phasor at each point $P(x, y, z)$ of space.

In a multiple antennas system, the total electric field phasor is written as follows:

$$\mathbf{E}(x, y, z) = \sum_{i=1}^N w_i \mathbf{E}_i(x, y, z) \left[\frac{\text{V}}{\text{m}} \right] \quad (2)$$

where \mathbf{E}_i and w_i are the individual electric field and excitation weights corresponding to each antenna of the transmission system respectively. In what follows, the (x, y, z) notation is assumed for all the electric fields and is removed for simplicity.

In most practical cases, the excitation of a MIMO system is exclusively simultaneous and the power is uniformly distributed between all the antennas. In this case, the SAR value for any arbitrary configuration of the MIMO system (defined by the excitation weights w_i) can be obtained by performing the following steps:

- Step#1: Perform N measurements of the electric field phasor $\mathbf{E}_m^{meas} = \sum_{i=1}^N w_{mi} \mathbf{E}_i$ (with $m=1, \dots$) for MIMO configurations with exclusively simultaneous excitations (i.e: $w_{mi} \neq 0, \forall m, i \in \{1, \dots\}$). w_{mi} is the excitations weight of the i^{th} MIMO antenna used for the m^{th} measurement.

In theory, these N measurements are sufficient for the retrieval of the electric fields \mathbf{E}_i corresponding to each individual antenna of the system, and thus the electric field and SAR values of all the MIMO excitation schemes [7]. These individual fields are obtained from the following equation:

$$\begin{bmatrix} \mathbf{E}_1 \\ \mathbf{E}_2 \\ \vdots \\ \mathbf{E}_N \end{bmatrix} = \mathbf{W}^{-1} \begin{bmatrix} \mathbf{E}_1^{mes} \\ \mathbf{E}_2^{mes} \\ \vdots \\ \mathbf{E}_N^{mes} \end{bmatrix} \quad \text{with } \mathbf{W} = \begin{pmatrix} w_{11} & \dots & \dots \\ \vdots & \ddots & \vdots \\ w_{N1} & \dots & \dots \end{pmatrix} \quad (3)$$

In practice, especially in the specific case of active MIMO antenna systems, there is no practical access to the antenna source-signals. Let us consider the ART-MANTM [10-11] system that takes measurements of the planar near-field vector phasor thanks to implementing a phase-coherent acquisition of the RF time-domain voltages induced, on one hand on, the scan probes, and on the other hand, on a fixed-

location probe that serves as the phase reference during a complete field scan.

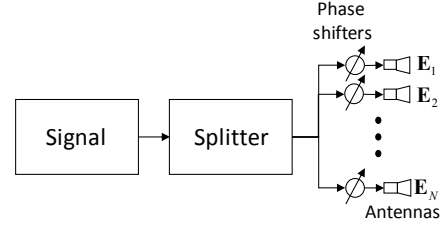


Fig. 1. MIMO communication system.

It is evident that from one field scan to the other in Step#1, the phase reference undergoes a shift that is introduced by the change in the illuminating field topologies in an unpredictable manner. Hence, it is generally not simple to define an independent phase reference for all the measurements of Step#1. As a result, equation (3) is not generally valid and additional “test” measurements are required in order to align the phase references of all of the N measurements.

- Step#2: Perform at least one “test” measurement $\mathbf{E}_m^{test} = \sum_{i=1}^N w_{ti} \mathbf{E}_i$ with excitation weights different from the ones used in Step#1.
- Step#3: Use the fields measured in Step#1 and Step#2 in order to calibrate and to align the phase reference of the different measurements. This is achieved by introducing a set of phase shifts β_m (with $m=2, \dots$) on the measured fields \mathbf{E}_m^{meas} and by minimizing the following cost function:

$$f(\beta_2, \dots) = \left\| \sum_{x,y,z} \left| \mathbf{T} \mathbf{W}^{-1} \begin{bmatrix} \mathbf{E}_1^{mes} \\ \mathbf{E}_2^{mes} e^{j\beta_2} \\ \vdots \\ \mathbf{E}_N^{mes} e^{j\beta_N} \end{bmatrix} \right|^2 - \sum_{x,y,z} |\mathbf{E}_m^{test}|^2 \right\| \quad (4)$$

where

$\mathbf{T} = [w_{t1} \dots]$ contains the excitation weights of the test measurement \mathbf{E}_m^{test} .

- Step#4: Retrieve the electric field \mathbf{E}_i corresponding to each individual antenna of the MIMO system as follows:

$$\begin{bmatrix} \mathbf{E}_1 \\ \mathbf{E}_2 \\ \vdots \\ \mathbf{E}_N \end{bmatrix} = \mathbf{W}^{-1} \begin{bmatrix} \mathbf{E}_1^{mes} \\ \mathbf{E}_2^{mes} e^{j\beta_2^{min}} \\ \vdots \\ \mathbf{E}_N^{mes} e^{j\beta_N^{min}} \end{bmatrix} \quad (5)$$

where (β_2^{min}, \dots) is the solution giving the minimum of $f(\beta_2, \dots)$.

It should be noted that the phase reference of the first measurement is arbitrarily considered here as a reference for the phase alignment in the formulations of equations (4) and (5) (i.e: $\beta_1 = 0$).

- Step#5: Compute the electric field \mathbf{E} corresponding to any relevant MIMO excitation scheme using equations (5) and (2).
- Step#6: For each MIMO configuration, compute the peak volume-averaged SAR of the system [4-8] for the compliance assessment purpose.

III. NUMERICAL AND EXPERIMENTAL VALIDATION

In order to validate the proposed method, two different MIMO scenarios were considered for a numerical and an experimental validation, respectively. The numerical simulations were performed on a FDTD model and the experimental measurements were obtained using the vector probe array measurement system ART-MANTM [10-11].

A. Numerical validation

For this numerical validation, a four antenna MIMO system composed of PIFA antennas was designed (see Fig.2) to operate at 1.9GHz. The antenna is placed at a distance of 10mm above a phantom of relative permittivity $\epsilon'_r = 40$ and electric conductivity $\sigma = 1.4$ [S/m] [2].

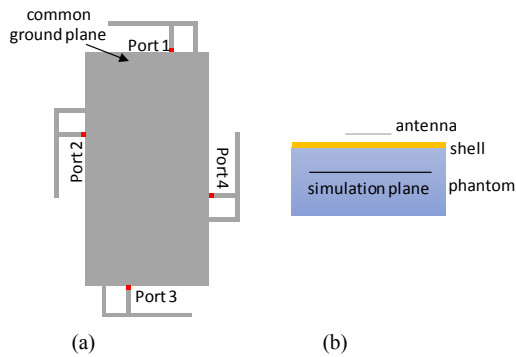


Fig. 2. Description of the simulation setup. (a) Top view of the antenna system. (b) Side view of the simulation setup.

Four sets of numerical simulation data were generated for various simultaneous unit excitation weights (Step#1). A random phase offset was introduced in the simulations in order to reproduce the arbitrary differences of the phase references between the measurements. An additional simulation was performed for phase alignment, according to Step#2. The applied different phase shifts of the MIMO antennas are summarized in Table.I. For the first phase configuration of this table, the amplitude and phase of simulated electric field are represented in Fig.3 at a distance of 20 mm inside the flat phantom (see Fig.2).

TABLE I. PHASE SHIFT EXCITATION OF THE MIMO ANTENNAS FOR THE SIMULATION SCENARIOS.

Simulation	Phase shift excitation (°)
------------	----------------------------

number	PIFA 1	PIFA 2	PIFA 3	PIFA 4
1	-95	155	145	-80
2	155	95	-150	95
3	-10	50	175	160
4	80	0	155	-145
5	70	100	5	50

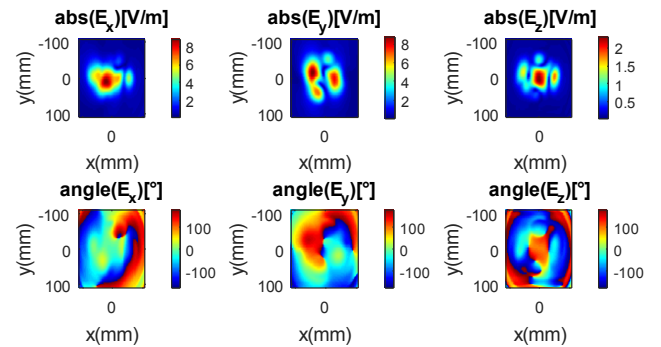


Fig. 3. Simulated electric field components at a distance of 20mm inside the phantom. The simulations were obtained with the first excitation phase values of table.I.

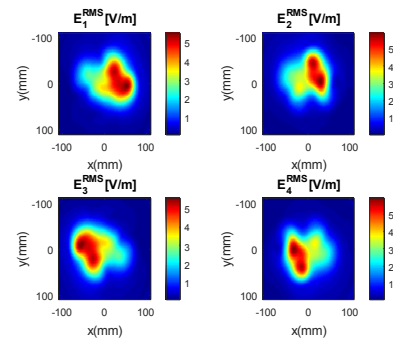


Fig. 4. Retrieved RMS value of the electric field corresponding to each antenna of the MIMO system.

The procedure described in section II was then performed on the five generated fields in order to retrieve the electric fields corresponding to each individual antenna of the MIMO system. A particle swarm optimization (PSO) algorithm was used in order to minimize the cost function of equation (4) and align the phases of the four simulations. The execution time of the optimization algorithm is 23s. The root mean square (RMS) value of the retrieved electric field is given in Fig.4. On the other hand, Fig.5 gives the simulated RMS value of the electric field obtained by separately exciting the four antennas. It can be seen from the two figures that the simulated and the retrieved electric field of the four antennas are identical. The retrieved fields of the MIMO antennas can then be combined using equation (5) in order to obtain the electric field and average SAR value of any desired MIMO excitation scheme.

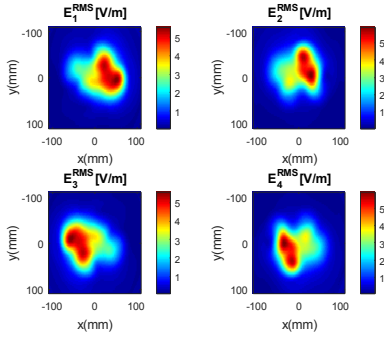


Fig. 5. Simulated RMS value of the electric field obtained by separately exciting each antenna of the MIMO system.

B. Experimental validation

The MIMO scenario considered for the experimental validation consists of two dipole antennas operating at a frequency of 1.9 GHz. The two dipoles are placed above an ART-MAN's flat phantom (vector probe array SAR measurement system) at a separation distance of 15mm (see Fig.6). The distance between the centers of the two dipoles is 0.5λ . The orientations of the two dipoles are 0° and 45° respectively. A controlled input power of 17dBm is injected in the two dipoles using two synchronized signal generators: a Rohde & Schwarz SMB 100A and an Agilent EXG N5172B. The phase shift of the two signals is controlled using local oscillator synchronization of the generators.

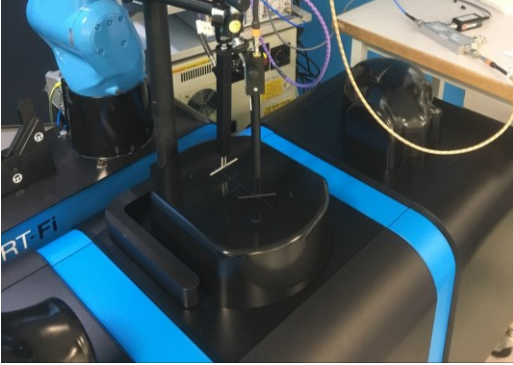


Fig. 6. Photography of the experimental validation set-up. Two dipole antennas placed above a flat phantom of ART-MAN (Vector array SAR measurement system)

TABLE II. PHASE SHIFT EXCITATION OF THE MIMO ANTENNAS FOR THE MEASUREMENTS

Measurement number	Phase shift excitation ($^\circ$)	
	Dipole 1	Dipole 2
1	0	-90
2	0	135
3	0	90

The two dipoles were excited using exclusively simultaneous excitations in order to perform two initial measurements of the electric field (Step#1) and a third additional test measurement for phase alignment (Step#2).

The phase excitations of the two antennas for the three measurements are given in Table.II. The measured tangential electric-field phasor at the probe plan corresponding to the first scenario of Table.II is given in Fig.7.

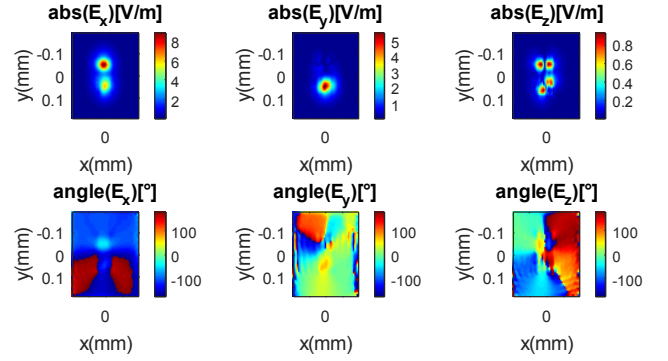


Fig. 7. Measured electric field components at a distance of 20mm inside the phantom. The measurement obtained using an ART-MAN system corresponds to the first phase excitation scheme of table.II.

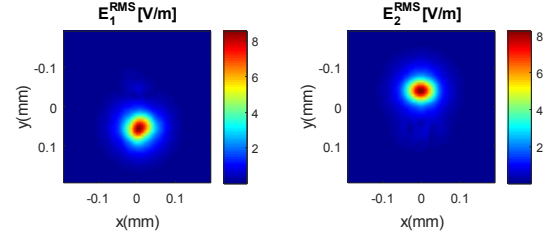


Fig. 8. Retrieved RMS value of the electric field of each Dipole antenna of the MIMO system.

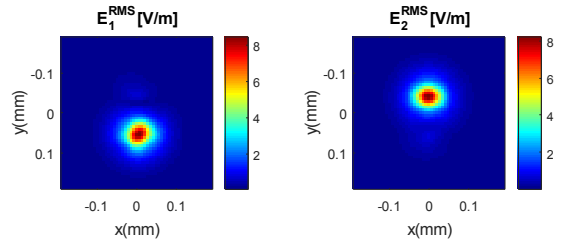


Fig. 9. Measured RMS value of the electric field obtained by separately exciting each Dipole of the MIMO system.

The proposed method was then performed on the three measurements in order to retrieve the electric field corresponding to each individual dipole of the system. The retrieved field RMS value is given in Fig.8. A PSO algorithm was used in order to minimize the cost function with an execution time of 20s. The two dipoles were then excited separately in order to measure the electric field corresponding to each one of them. The RMS value of the measured fields are represented in Fig.9. It can be seen from the two figures that distributions of the measured individual fields and those of the retrieved fields of two antennas are in very good agreement, with a Normalized Root Mean Square Error (NRMSE) of 2.9%.

The two retrieved complex phasors of the electric-fields were then combined in order to obtain the total electric field vector and peak volume-averaged SAR values corresponding to any excitation scheme of the MIMO system. A comparison between the retrieved (blue) and measured (red) SAR 1g and 10g values are represented in the Fig.10 and Fig.11 respectively. A third curve (green) is reported to represent conservative SAR value that one obtains if only the amplitude of the E-fields is measured and combined for the evaluation of over-estimate SAR. It can be seen from the two figures that a very good agreement (less than 3.5% error) was obtained between the retrieved and measured SAR values. In addition, the true (exact) SAR value is strictly up to 15% smaller than the conservative SAR value.

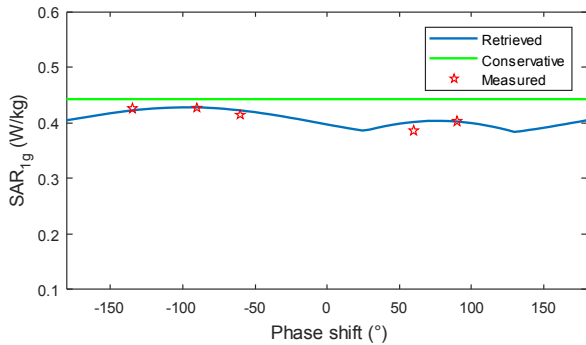


Fig. 10. Comparison between the retrieved (blue), the conservative (green) and the measured (red) SAR 1g values.

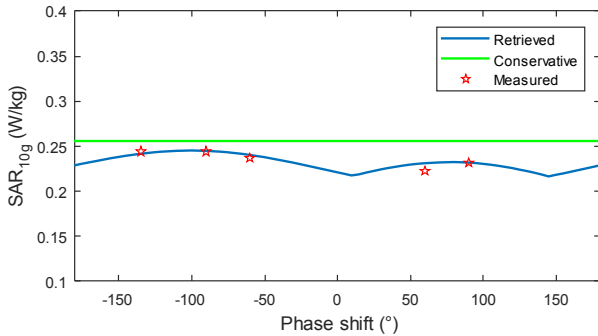


Fig. 11. Comparison between the retrieved (blue), the conservative (green) and the measured (red) SAR 10g values.

IV. CONCLUSION

In this paper, an efficient method for the rigorous evaluation of true SAR values of MIMO devices is presented. The proposed method is particularly adapted to the case of exclusively simultaneous excitation schemes of active MIMO systems. Rigorous SAR evaluation allow for the enhancement of communication devices by alleviating the strict constraints on exposure level caused by the SAR over-estimation of classical methods. The proposed method uses as few as $N+1$ measurements for an N antenna system in order to retrieve the SAR for all the possible excitations schemes of the MIMO system. The efficiency of the

proposed method is enabled thanks to the use of radio-frequency vector-probe system to take direct measurements of the amplitude and phase of the electric field phasor.

V. ACKNOWLEDGEMENT

This project (16NRM07) has received funding from the EMPIR programme co-financed by the Participating States and from the European Union's Horizon 2020 research and innovation programme.

REFERENCES

- [1] Z. Ying, "Antennas in cellular phones for mobile communications," *Proc. IEEE*, vol. 100, no. 7, pp. 2286-2296, Jul. 2012.
- [2] Measurement procedure for the assessment of specific absorption rate of human exposure to radio frequency fields from hand-held and body-mounted wireless communication devices - Part 3: Vector measurement-based systems (Frequency range of 600 MHz to 6 GHz), 1st ed., *Standard IEC 62209-3*, 2019.
- [3] ICNIRP Guidelines Draft Ed. (2018). Draft Guidelines for Limiting Exposure to Time-Varying Electric, Magnetic, and Electromagnetic Fields (up to 300 GHz). [Online]. Available: <https://www.icnirp.org/en/activities/public-consultation/consultation-1.html>
- [4] B. Thors, D. Colombi, Z. Ying, T. Bolin, and C. Tornevik, "Exposure to RF EMF from array antennas in 5G mobile communication equipment," *IEEE Access*, vol. 4, pp. 7469-7478, 2016.
- [5] "Guidance for evaluating exposure from multiple electromagnetic sources," *IEC, Tech. Rep.* 62 630, Oct. 2010.
- [6] N. Perentos, S. Iskra, A. Faraone, R. J. McKenzie, G. Bit Babik and V. Anderson, "Exposure Compliance Methodologies for Multiple Input Multiple Output (MIMO) Enabled Networks and Terminals," *IEEE Transactions on Antennas and Propagation*, vol. 60, no. 2, pp. 644-653, Feb. 2012.
- [7] B. Xu, M. Gustafsson, S. Shi, K. Zhao, Z. Ying and S. He, "Radio Frequency Exposure Compliance of Multiple Antennas for Cellular Equipment Based on Semidefinite Relaxation," in *IEEE Transactions on Electromagnetic Compatibility*, vol. 61, no. 2, pp. 327-336, April 2019.
- [8] D. T. Le, L. Hamada, S. Watanabe and T. Onishi, "A Fast Estimation Technique for Evaluating the Specific Absorption Rate of Multiple-Antenna Transmitting Devices," in *IEEE Transactions on Antennas and Propagation*, vol. 65, no. 4, pp. 1947-1957, April 2017.
- [9] R. Meyer, S. Kühn, K. Pokovic, F. Bomholt and N. Kuster, "Novel Sensor Model Calibration Method for Resistively Loaded Diode Detectors," in *IEEE Transactions on Electromagnetic Compatibility*, vol. 57, no. 6, pp. 1345-1353, Dec. 2015
- [10] B. Derat, L. Aberbour and A. Cozza, "Near-field and vector signal analysis techniques applied to specific absorption rate measurement," 2015 IEEE MTT-S 2015 International Microwave Workshop Series on RF and Wireless Technologies for Biomedical and Healthcare Applications (IMWS-BIO), Taipei, 2015, pp. 34-35.
- [11] ART-MAN [Online]. Available: <http://www.art-fi.eu/sar/solutions/sar-measurement-system>
- [12] L. Aberbour, O. Jawad, M. Ramdani, P. Giry and T. Julien, "Efficient Experimental Assessment of The Specific Absorption Rate (SAR) Induced by MIMO Wireless Communication Devices; Application of Vector Near-Field Measurement System," *2018 IEEE Conference on Antenna Measurements & Applications (CAMA)*, Vasteras, 2018, pp. 1-4.